An Experimental Study of the Shock Structure in a Partially Ionized Gas

R. H. KIRCHHOFF* AND L. TALBOT†
University of California, Berkeley, Calif.

Shock structure experiments were carried out in a radio-frequency-heated, steady-state, low-density, partially-ionized argon plasma jet. The primary diagnostic tool was a cylindrical free molecule Langmuir probe aligned with the flow, which was used to probe a normal shock wave. Spatial resolution was 13% of the heavy-particle shock thickness; thus, details of electron temperature, ion number density, and plasma potential were obtained through the shock. The electron temperature rise was observed to precede the heavy-particle shock. The plasma potential converted from floating potential according to the theory of Laframboise was in substantial agreement with changes in plasma potential obtained from a numerical quadrature of the generalized Ohm's law assuming zero current. An explanation of the dark space observed to precede partially ionized gas shocks is provided by comparing the collisional-radiative recombination rate calculated with observed electron temperature and number density to the luminosity of the flow. The integration of the electron energy equation, including the effect of recombination energy transfer, was found to be in substantial agreement with the data.

Nomenclature

a,b,c = constants in the electron energy equation defined in Sec. 7
d = maximum slope thickness of atom shock
D = diameter of nozzle throat or freejet orifice
D_i = ion diffusion coefficient
D_a = ambipolar diffusion coefficient, $D_a = D_i[1 + (T_e/T_i)]$
e = electronic charge
$\mathbf{E}$ = electric field
ev = electron volt
K_e = electron thermal conductivity
k = Boltzmann's constant
l = cylindrical probe length
m = species mass
$\dot{m}$ = mass flow rate
M = Mach number
n = species number density
p = species pressure
q_e = energy transfer of recombination
r,r_p = probe radius
Re_D = throat Reynolds number
$Sc_{i,a}$ = Schmidt number = $Sc = \mu/\rho D_{i,a}$
T = species temperature
V = potential
V_0 = plasma potential
V_f = probe floating potential
V_g = ground potential
V_p = probe potential
x = axial distance
α = recombination coefficient
Δ = thermal layer thickness
ϵ = energy given to the electron gas per recombination
λ_D = Debye length
λ_{ij} = mean free path for species i scattered by species j
Λ = $12\pi n_e\lambda_D^3$
μ = viscosity
ξ = x/d
ρ = mass density
τ = $T_{e\infty}/T_{a\infty}$
τ' = $T_{e\infty}/T_{a2}$

Subscripts

0 = stagnation
∞ = freestream
i = ion
e = electron
n = neutral
p = probe
a = atom, ambipolar
1,2 = upstream and downstream of the shock, respectively

Presented as Paper 69-697 at the AIAA Fluid and Plasma Dynamics Conference, San Francisco, Calif., June 16–18, 1969; submitted July 14, 1969; revision received July 21, 1970. This research was supported by the Air Force Office of Scientific Research under AFOSR Grant 538-67.

* Research Assistant; presently Assistant Professor, University of Massachusetts, Amherst, Mass. Member AIAA.
† Professor of Aeronautical Sciences. Member AIAA.

1. Introduction

A STRIKING visual feature of low-density supersonic plasma afterglows is the dark space which occurs upstream of the luminous shock front formed ahead of a body immersed in the otherwise completely luminous plasma flow. It has been suggested[1] that this dark space is due to a region of elevated electron temperature that occurs ahead of the shock front in such flows.

Several analyses[1,2] have been carried out on the structure of shock waves in partially ionized gases. The problem can be viewed in terms of a two-fluid model, one fluid composed of electrons, the other composed of atoms and ions. Separate shocks are formed in the two fluids, but they are coupled by electrostatic and dissipative forces. The analyses predict, among other things, two physical phenomena that are pertinent to the present investigation. First, the electron temperature is found to rise upstream of the heavy-particle shock on a length scale many times that of the heavy-particle shock. This result is attributed to a very high electron-gas conductivity, coupled with the thermal isolation of the electron gas from the heavy-particle gas. Second, an electric field, and thus an associated change in plasma potential, is predicted to occur through the body of the shock. The electric field arises due to the retarding Coulomb force, which opposes the tendency for the electrons to diffuse relative to the ions in the presence of the shock gradients.

Christiansen[3] studied experimentally the shock structure in front of a flat disc in a supersonic seeded-gas plasma. He measured the recombination radiation of the diffuse series limit of cesium, from which he obtained the electron temperature. He observed the elevated electron temperature in front of the shock and correlated his results with the Spitzer model of electron thermal conductivity. Because of the resolution of the experiment, which was of the order of the

heavy-particle shock thickness, no detailed measurements were made of the heavy-particle shock itself. The dark space was observed in front of the shock, but no quantitative explanation for it was given. Sonin[4] used a Langmuir probe operating under free-molecule conditions to obtain electron temperature and ion saturation-current density surveys through a blunt body stagnation layer and through a shock wave formed in a freejet. No change in electron temperature was observed in either case; however, considerable diffusive broadening of the ion number-density shock wave profiles was observed. These measurements were made in a highly nonequilibrium flow in which $T_{e\infty}/T_{a\infty} \equiv \tau \simeq 15$. Kamimoto, Nishida, and Yoshida[5] also carried out theoretical and experimental studies of the highly nonequilibrium, partially ionized gas shock wave. Their results show that when $\tau' = T_{e\infty}/T_{a2}$ is of order one or more, the electron temperature is unchanged through the shock ($\tau' \sim 1$) or merely relaxes the atom temperature ($\tau' > 1$). Langmuir probe electron temperature measurements, which are in agreement with theory, are presented in Ref. 5. The dark space was also observed in this experiment, although again, an explanation for it was not provided.

The present paper describes the results of a laboratory experiment performed with the objective of measuring the electron temperature, the electric field, and the ion number density within a shock wave produced in a low-density partially ionized flow. The primary diagnostic tool used was a cylindrical Langmuir probe aligned with the flow direction and operated under collisionless flow conditions. The data were used with a recombination theory to provide a quantitative explanation for the dark space. A computer experiment involving the electron energy equation was also performed to elucidate the role of the recombination process in the electron energy balance through the shock wave.

2. Experimental Apparatus

The experiments described in this report were performed in an rf-heated, low-density plasma tunnel which is part of the Rarefied Gas Dynamics Facility at Berkeley. Argon gas was ionized by radio-frequency induction at 4 MHz and expanded through either a nozzle or a freejet. The properties of these flows are given in Table 1. Details of the wind tunnel and its associated instrumentation have been reported elsewhere.[6]

3. Flow Properties

Impact pressure surveys made along the centerline of the freejet flow were found to be in excellent agreement with the fitting formula of Ashkenas and Sherman.[7] This fact is taken to imply that the neutral particle density in the jet is proportional to $(x/D)^{-2}$. The jet Mach number as a function of x/D was estimated from the theory of Sherman[8] for $\gamma = \frac{5}{3}$ with his viscous correction employed. The jet had an exit-plane to Mach-disk distance of 11 in. and Mach disk diameter of over 5 in. Radial surveys in the freejet show that the impact pressure, charged-particle number density, and electron temperature have only a very small variation in front of the shock. This is desirable for comparison to one-dimensional shock theory. Calculations of the electron collision frequency in the jet show that electron-ion collisions are dominant. This implies that the electron transport properties may be approximated by fully ionized gas theory.

The luminosity in the jet and in the nozzle flow results from the recombination process. The predominant mechanism is the electron-electron-ion three-body recombination to an excited atomic state followed by collisional and radiative de-excitation to the ground state.[9,10] In this process part of the energy is given to the free electron through inelastic (super-elastic) collisions. The over-all process may be represented as

$$A^+ + e + e \rightarrow A_m + e$$

followed by the two competing de-excitation processes

$$A_m + e \rightarrow A_n + e$$

(electron super-elastic collisional de-excitation)

$$A_m \rightarrow A_n + h\nu_{mn} \text{ (radiative de-excitation)}$$

The energy transfer to the electrons associated with the super-elastic collisions is generally non-negligible in the over-all energy balance. This energy transfer is introduced into the electron energy equation in Sec. 7.

The rate of recombination is calculated most conveniently from the theory of Hinnov and Hirschberg[9] and is small enough that the charged particle number density should also be proportional to $(x/D)^{-2}$. The experimental results were found to agree with this prediction.

The nozzle-expanded flow was found to have radial gradients in the impact pressure and the charged particle number density. However, visual observation indicated that the shock was relatively flat. The previous comments about recombination and the electron-ion collision frequency also apply to the nozzle-expanded flow.

Table 1 Flow conditions[a]

	Nozzle flow	Freejet
$\dot{m}$, g/sec	0.43	1.41
T_0, °K	2000	1240
P_0, torr	5	9.3
P_{static}, torr	0.030	0.090
T_{static},[b] °K	1000	53
λ_{nn_∞},[b] cm	0.7	0.20
λ_{in_∞},[b] cm	0.334	0.355
r_p/λ_D	$80 \leq r_p/\lambda_D \leq 100$	$20 \leq r_p/\lambda_D \leq 50$
α,[b] $(\text{cm}^3/\text{sec})^{-1}$	4×10^{-10}	1.65×10^{-11}
λ_{ei_∞},[b] cm	0.0116	0.274
Re_D	176	809

[a] All these flows were produced with a nozzle throat or an orifice diameter of 1.75 in.
[b] In the freejet, this refers to the minimum density point ahead of the Mach disk.

4. Langmuir Probe Measurements in a Flowing Plasma

Because of its excellent spatial resolution and its relatively simple construction, the Langmuir probe is an attractive diagnostic instrument for low-density plasma flows. Excellent reviews of Langmuir probe theory are available in Loeb[11] and Chen.[12] The most complete treatment of the theory for probes operated under collisionless conditions is given by Laframboise.[13]

The Langmuir probes used in this study were of the cylindrical double and single type. Typical probes were fabricated of tungsten wire with a diameter of 0.005 in. or 0.010 in. and aspect ratios $l/r \simeq 40$. The construction and cleaning of the probes were found to be crucial to their proper operation and to the reproducibility of results. In particular, it was found that reproducibility of results was greatly enhanced if, before measurements were made with a probe, it was ion-sputtered in its operating plasma environment. Details of probe construction, operation, and electronic circuitry are given in Refs. 14 and 15.

In order that collisionless probe theory be applied it is necessary that all relevant mean free paths be much greater than the probe diameter. The probe diameter used in these experiments was 0.025 cm. A comparison between this dimension and the appropriate free paths listed in Table 1 and Fig. 1 shows that collisionless conditions were not achieved in all cases.

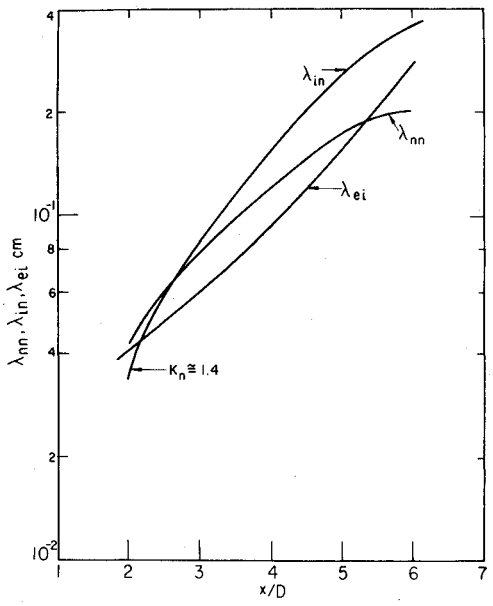

Fig. 1 Mean free paths in the freejet.

In the nozzle flow experiment the freestream electron-ion Knudsen number $\lambda_{ie}/2r_p$ is 0.46. It was found that single-probe retarding field electron current measured by a pulsed technique exhibited collisional effects.[15] For this reason only the double-probe technique was used to measure electron temperature in the nozzle experiment, since it has been shown[15] that under conditions where collisional effects render useless the electron temperature measurement by single probes, double probes can still be used for electron temperature determination. In the freejet flow the minimum electron-ion Knudsen number is large enough that collisional effects on the single probe electron current measurements are not observed.

Ion-neutral collisions are predominantly responsible for collisional effects on the ion current observed in the freejet flow.[14] In the nozzle flow experiment the freestream ion-neutral Knudsen number $\lambda_{in}/2r_p$ is 13, and aft of the shock it is 6. Thus no significant collisional effects on the ion current due to ion-neutral collisions are expected in the nozzle flow. However, some collisional effect on the ion current due to electron-ion collisions may be present in the nozzle experiment. But in the absence of a useful theory accounting for such collisional effects, no corrections to the data were made.

All ion number densities were determined from the ion saturation current using the theory of Laframboise.[13] The plasma potential was not measured directly, but was determined by two independent techniques. One technique was to convert the measured floating potential V_f to the plasma potential using the theory of Laframboise, which accounts for the effect of the ratio of probe radius to Debye length and ratio of ion to electron temperature.

The other technique was to obtain the plasma potential from an integration of the generalized Ohm's Law, assuming zero current. For zero current and no magnetic field, the generalized Ohm's Law may be written

$$\mathbf{E} = -(1/n_e e)\nabla p_e - (\beta k/e)\nabla T_e$$

where for predominantly electron-ion collisions β may be taken as $\frac{3}{4}$.[16] The definition of electric potential, together with Ohm's Law and measurements of electron temperature and number density, are sufficient to calculate changes in potential. Changes in plasma potential through the shock waves calculated in this fashion will be compared to changes in plasma potential inferred from changes in floating potential.

5. Nozzle Flow Experiment

Figure 2 shows a photograph of the flow with the shock holder in place. The dark space in front of the shock is quite evident; when the shock holder is removed, the flow is continuously luminous in the region where the dark space occurs and also far downstream of this region. Figure 3 shows ion number density n_i and electron temperature T_e vs position starting from the nozzle exit plane and extending through the shock holder. The density ratio across the ion shock is 2.25, which corresponds to a Mach number of 1.96 and a heavy-particle temperature ratio of 2.04. The maximum slope thickness of the ion density profile is 3.68 cm.

To compare this shock thickness with theory, we note that the data of Robben and Talbot[17] in the region of $M = 2$ fall very close to the Mott-Smith estimate of shock thickness. At Mach number 2, the Mott-Smith theory gives $\lambda_\infty/d = 0.21$. The freestream atomic temperature in the flow under study has been found by electron beam measurements to be approximately 1000°K.[18] At the measured chamber static pressure of 0.034 torr, this temperature yields an atom-atom free path of 0.7 cm and thus a measured λ_∞/d of 0.19. This close correspondence is taken as partial evidence that there is negligible diffusive separation between ions and atoms in this shock wave.

Sinclair et al.[19] calculated diffusive separation as a function of ambipolar Schmidt number $Sc_a = \mu/\rho D_a$ in a partially ionized argon shock at Mach number 2.2 and $T_0 = 450$°K. They predict the onset of diffusive separation to occur at $Sc_a \lesssim 0.4$. Since the equilibrium Schmidt number scales approximately as the fourth root of the temperature, the conditions in this experiment would indicate the onset of diffusive separation at $Sc_a \lesssim 0.56$. The ambipolar Schmidt number calculated for this experiment is $Sc_a = 2.2$. This is taken

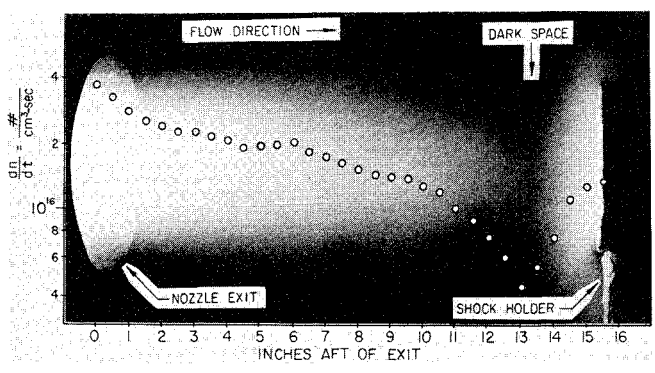

Fig. 2 Nozzle flow and shock holder with recombination rate superimposed.

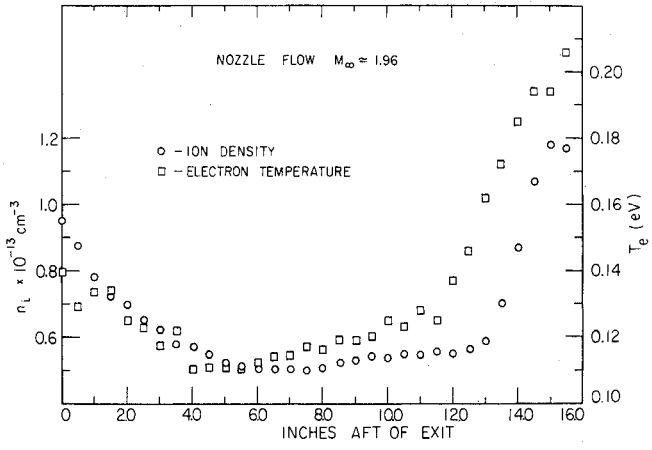

Fig. 3 Axial electron temperature and ion number density.

as further evidence that diffusive separation is not to be expected in this experiment.

Axial surveys of electron temperature and ion number density in the nozzle flow shock are shown in Fig. 3. The most striking feature of the profiles is that the rise in electron temperature precedes the ion shock. Since the flow from the conical nozzle is not uniform and because there is some scatter in the electron temperature data, it is difficult to choose the point upstream of the shock where the electron temperature asymptotically approaches its freestream value and is no longer affected by the shock. For the purpose of discussion, this point will be taken at 8.5 in. downstream of the nozzle exit plate at an electron temperature $T_e = 0.119$ ev. The corresponding value of τ is 1.38. The distance from the center of the ion shock to this point will be called Δ, the thermal thickness. It is unfortunate that in none of the existing analyses is an example calculated which is close enough to our experimental conditions to make possible a proper comparison between theory and experiment for Δ/d, the ratio of the thermal thickness to the shock thickness. Our measurements yielded $\Delta/d \simeq 3.4$. The results of our numerical integration of the electron energy equation with recombination energy transfer for the conditions of this experiment are presented in Sec. 7. We found from the calculations the value $\Delta/d \simeq 3.0$, which is in very reasonable agreement with the measured value.

The theoretical atom temperature ratio across the shock at a Mach number of 1.96 is 2.04, whereas the measured electron temperature ratio was found to be 1.68. Although the atomic temperature ratio is higher, the postshock electron temperature is still greater than the postshock atom temperature, as would be expected in a recombining plasma. A calculation (see Sec. 7) of the upstream and downstream electron energy balance performed by equating the collisional energy transfer between ions and electrons to the recombination energy transfer shows that electron temperature ratio across the shock should be 1.63, whereas the measurements yielded a ratio of 1.68. The measurement of the postshock electron temperature had a 6% scatter and was made at one ion-shock thickness downstream of the center of the ion shock.

As was mentioned earlier, the striking visual feature of the flow is the dark space that occurs upstream of the luminous shock front, as seen in Fig. 2. It has been suggested[1] that the dark space is due to the region of elevated electron temperature ahead of the shock front and comes about because of the strong inverse dependence of the recombination rate on the electron temperature, and because the luminosity of the flow is proportional to the recombination rate. A calculation of the recombination rate using experimentally determined values of the electron temperature and number density should provide a test of this hypothesis.

The recombination rate according to the collisional-radiative model of recombination from the theory of Hinnov and Hirschberg[9] is given as

$$(dn_e/dt)_{\text{recomb}} = -5.6 \times 10^{-27} n_e^3 \text{ cm}^3/T_e^{9/2}\text{sec}$$

where n_e is the electron number density per cm^3 and T_e is the electron temperature in electron volts. The electron temperature and charged-particle number density data of Fig. 3 were used to calculate $(dn_e/dt)_{\text{recomb}}$ along the axis of the jet, and the values thus obtained have been plotted on the photograph of the flow in Fig. 2. It is striking that the minimum in the recombination rate occurs at the point of minimum luminosity in the dark space, in accord with the hypothesis advanced in Ref. 1.

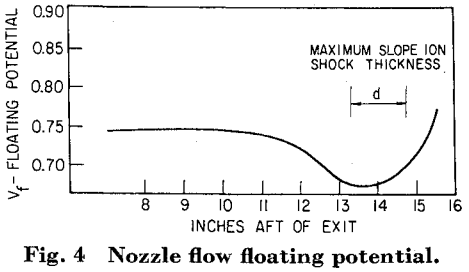

Fig. 4 Nozzle flow floating potential.

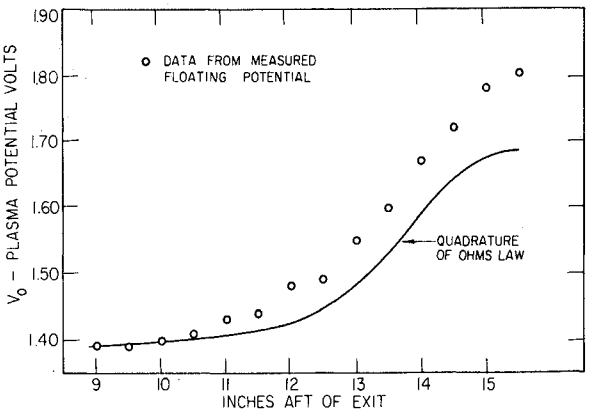

Fig. 5 Nozzle flow plasma potential.

Another of the objectives of the experiment was to measure the predicted electric field and corresponding change in plasma potential through the shock wave. Figure 4 shows the floating potential ahead of and through the shock wave. It will be noticed that V_f first drops before it rises through the shock. The drop is caused by the fact that in front of the ion shock, the increase in electron temperature moves the probe floating potential more negative relative to the plasma potential than the plasma potential itself is increased above ground potential by the same change in electron temperature. However, as the plasma potential begins to be affected by the ion shock, this trend is reversed and the probe floating potential increased.

Figure 5 shows the measured probe floating potential, converted through the use of the Laframboise results to plasma potential, compared to the plasma potential obtained by integrating the generalized Ohm's Law. These data are taken as evidence that an electric field does exist within the shock, that it is in the correct (upstream) direction, and that there is no current in the shock. The maximum electric field is $\mathbf{E} = -5$ v/m, with a measured change in plasma potential across the shock of 0.42 v.

The discrepancies between the data of Fig. 5 and the calculated results are believed to be due at least in part to a probe temperature effect that is not completely understood. It was found that if the probe was moved slowly through the shock wave, so as to permit it to be everywhere in approximate thermal equilibrium with the flow, the floating potential variation observed was different from that found when the probe was moved rapidly through the shock, and thus maintained more nearly at an isothermal condition. The most consistent data were obtained with very rapid traverses, and these are the data reported. The temperature effect was considerable; if, for example, the probe was moved rapidly through the shock and then allowed to come to thermal equilibrium downstream of the shock, the equilibration process was accompanied by an additional increase of about 0.2 v in the indicated floating potential. Since there was some heating of the probe even with the most rapid upstream-to-downstream traverses available to us, the probe potential data might be expected to lie above the calculated results, and in fact they do, as seen in Fig. 5.

A calculation of the energy stored in the electric field is of interest. This energy is given by

$$W = \tfrac{1}{2}\epsilon_0 E^2 \qquad \text{(M.K.S.)}$$

where W is the stored energy in the field. At the point of

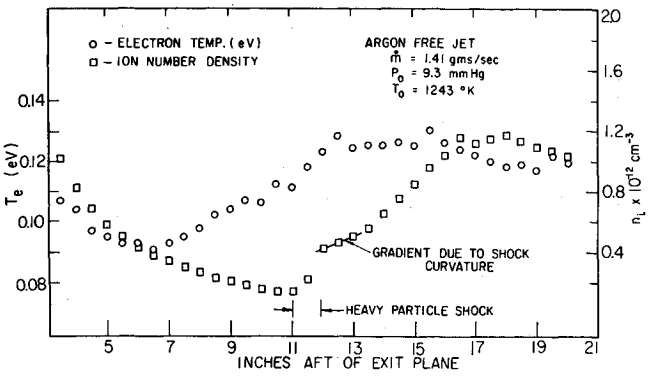

Fig. 6 Electron temperature and ion density in freejet.

maximum field strength $\mathbf{E} = -5$ v/m and $W = 2.71 \times 10^{-12}$ joules/m^3. At the same point in the shock, the internal energy of the electron gas $U_e = (\frac{3}{2})n_e k T_e = 3.26 \times 10^{-1}$ joules/m^3. Thus a negligible fraction of the energy of the electron gas is stored in the field.

Since the electric field is due to the charge separation, it is of interest also to calculate the charge separation $n_i - n_e$ from Poisson's equation

$$\nabla \cdot \mathbf{E} = e/\epsilon_0(n_i - n_e) \qquad \text{(M.K.S.)}$$

The charge separation is zero upstream and downstream of the shock, and at the point of maximum $\mathbf{E}$. The maximum charge separation occurs downstream of the center of the shock, at about 14.6 in. downstream of the exit plane, where it has a value of $n_i - n_e = 0.87 \times 10^{10}$m^{-3} and a corresponding percentage charge separation of 8.14×10^{-8}%. Thus, as is well known, an extremely small charge separation can produce a measurable electric field.

The effect of the finite rate of recombination on the shock profile can be estimated by comparing $(dn_e/dt)_{\text{rec}}$ with $u\partial n_e/\partial x$. In this case the recombination rate is 8% of the product of the measured maximum ion density gradient and the velocity at that point in the shock. Thus, we may consider the ion density to be frozen.

6. Freejet Experiment

In this jet the stagnation pressure was measured and the neutral particle density along the jet axis was measured in the freejet using electron beam technique.[18] The neutral argon temperature was calculated from the viscous correction given by Sherman.[8] The appropriate mean free paths are graphed in Fig. 1.

Figure 6 is a plot of charged-particle number density and electron temperature vs position in the freejet. The minimum ion number density occurs at 10.5 in. ($x/D = 6$), and the heavy-particle shock is in the region between 10.5 and 12.5 in. downstream of the exit plane. The measured maximum slope thickness based on the freestream mean free path at $x/D = 6$ is $\lambda/d \cong 0.19$. The isentropic Mach number at $x/D = 6$ is 10.6, and the Mach number based on the viscous correction of Sherman is 9.9. The Mott-Smith maximum slope thickness for argon at Mach number 9.9 is $\lambda/d = 0.18$. This excellent agreement is partly fortuitous because the ion number-density gradients upstream and downstream of the shock make it difficult to estimate maximum slope shock thickness. However, the indicated agreement is taken as partial evidence that there is no diffusive separation of ions and atoms in this shock. The ion density change across the shock was also difficult to estimate due to the same gradients; for the freejet shock we measured $n_2/n_1 \simeq 3.06$. Preliminary electron beam measurements[18] of the atom density in this jet also show that ion and atom shocks coincide, which is further evidence for the absence of diffusive separation. The ion Schmidt number $Sc_i = \mu/eD_i$ at $x/D = 6$ is 1.97; however, the ambipolar Schmidt number $Sc_a = \mu/eD_a$ is 0.073 at the same point because of the high degree of nonequilibrium. With so small an upstream ambipolar Schmidt number, one might be led to expect significant diffusive separation, contrary to the evidence. Perhaps a more appropriate criterion for predicting ion diffusive separation would be the ambipolar Schmidt number at the sonic point in the shock, which in the present case has the value 1.59.

It can be seen in Fig. 6 that the ion density profile rises slowly in the region along the axis between 12 and 13.5 in. from the nozzle exit, and then undergoes a much steeper rise in the region between 14 and 16.5 in. Robben and Talbot[17] give a relation for the density gradient behind a shock wave due to the flow divergence in the freejet and to shock curvature. The slope of the slowly rising profile in the region between 12 and 13.5 in. from the nozzle exit is accurately predicted by this relation. From the experiment the dimensionless density gradient is found to be equal to 3.06, whereas from the theory at Mach number 9.9 it is 2.95. The more steeply rising part of the density profile has a dimensionless gradient of about 9.7, considerably greater than the aforementioned theoretical prediction. The mechanism responsible for this increase in density gradient is not fully understood at this time. Preliminary neutral particle density measurements obtained by electron beam techniques[18] also exhibit this phenomenon.

The electron temperature rise extends over a quite broad region upstream of the atom shock. Without the competing mechanism of electron temperature decrease due to flow expansion the upstream boundary of the region of elevated electron temperature undoubtedly would have been much less well defined. At this shock Mach number the postshock atom temperature T_a is calculated to be 1170°K, which is less than the postshock electron temperature T_e of 1460°K, as it should be for a plasma with a finite recombination rate.

The plasma potential is given in Fig. 7. These data indicate the presence of an electric field not only in the interior of the shock but also in the source region and in the postshock region of the jet. It will be noted that here the probe potential data lie below the calculated plasma potential in the region downstream of the shock. The lack of agreement between the numerical quadrature of Ohm's Law and the plasma potential as calculated from the probe floating potential is believed to be here due mainly to the effect of collisions on the probe floating potential,[15] although compensated for in part by the thermal effect described earlier. In general, collisions tend to increase the value of probe floating potential above the collisionless value. The maximum value of the electric field in the shock is -5.9 v/m, and as in the case of the nozzle flow experiment, the percent charge separation and the stored energy in the field are extremely small.

As in the case of the nozzle flow, the dark space is evident in the photograph of the jet in Fig. 8, and the recombination

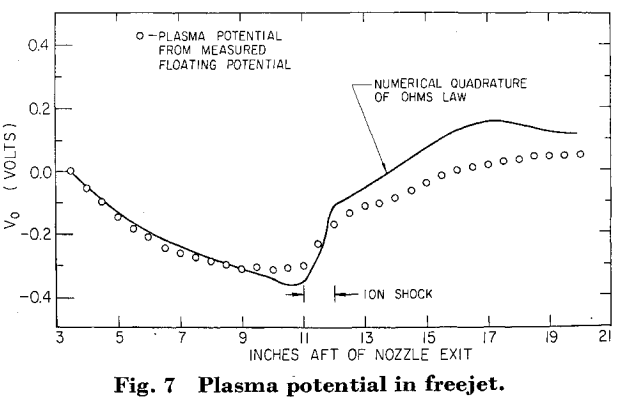

Fig. 7 Plasma potential in freejet.

rate dn_e/dt is found to exhibit a strong minimum just upstream of the atom shock.

7. The Computer Experiment

Although recombination can be neglected as unimportant with regard to the charged-particle density distribution in the flow, the recombination energy exchange in the electron gas is not negligible in the electron energy balance. None of the theories mentioned in Sec. 1 consider an electron energy equation that includes this process. In what follows, we consider the effect of this energy exchange on the electron temperature variation through the shock wave.

Following Jaffrin,[2] but adding a term for recombination energy transfer, we write the electron energy equation for a plane shock as

$$\frac{3}{2} C_e k \frac{dT_e}{dx} + C_e \frac{kT_e}{u_e} \frac{du_e}{dx} - \frac{d}{dx}\left(K_e \frac{dT_e}{dx}\right) = \xi_{ei} + q_e \quad (1)$$

where $C_e = n_e u_e$ is constant, T_e is the electron temperature, K_e is the electron thermal conductivity, k is Boltzmann's constant, ξ_{ei} is the electron-ion collisional energy transfer, and q_e is the energy transfer of recombination. We neglect electron-atom collisional energy transfer because it is negligible relative to ξ_{ei} and we assume that the ion and atom temperatures are the same. The latter collisional energy transfer is given by

$$\xi_{ei} = -4n_e(m_e/m_i)\nu_{ei}k(T_e - T_i) \quad (2)$$

where ν_{ei} is the electron-ion collision frequency as given in Holt and Haskell,[20]

$$\nu_{ei} = 2.63 n_i \ln\Lambda / T_e^{3/2} \text{ sec}^{-1}$$

Here n_i is in cm^{-3} and T_e is in °K;

$$q_e = -(dn_e/dt)\epsilon = \alpha n_e^2 \epsilon(n_e) \quad (3)$$

where dn_e/dt is the recombination rate and ϵ is the energy given to the electron gas per recombination. The value of α is taken from the theory of Hinnov and Hirschberg[9] as

$$\alpha = 10.5 \times 10^{-9} n_e/T_e^{9/2} \text{ cm}^3\text{sec}^{-1}$$

where T_e is in degrees Kelvin. The value of ϵ as a function of electron number density was taken from Chen,[10] for the case of an optically thin plasma.

We define the following dimensionless parameters

$$\theta = T_e/T_{e_\infty},\ \xi = x/d,\ \nu = n_e/n_{e_\infty},\ \phi = T_i/T_{e_\infty}$$

where the subscript ∞ refers to freestream properties. The energy equation may then be written as

$$\frac{d\theta}{d\xi} - \frac{2}{3}\frac{\theta}{\nu}\frac{d\nu}{d\xi} - \frac{2}{3}\frac{K_{e_\infty}}{C_{e_\infty}kd}\frac{d}{d\xi}\left(\theta^{5/2}\frac{d\theta}{d\xi}\right) = -\frac{8}{3}(2.63)\frac{n_{e_\infty}^2}{C_{e_\infty}} \times \frac{m_e}{m_i}\frac{\ln\Lambda_\infty}{T_{e_\infty}^{3/2}}\frac{\nu^2(\theta - \phi)}{\theta^{3/2}} + \frac{2}{3}\frac{10.5 \times 10^{-9} n_{e_\infty}^3 \epsilon d}{C_{e_\infty}kT_{e_\infty}^{11/2}}\frac{\nu^3}{\theta^{9/2}} \quad (4)$$

where $\ln\Lambda$ will be taken as constant at its upstream value $\ln\Lambda_\infty$.

For convenience we write

$$c = \tfrac{2}{3}\, 10.5 \times 10^{-9} n_{e_\infty}^3 \epsilon d / C_{e_\infty} k T_{e_\infty}^{11/2}$$

$$b = \tfrac{8}{3}(2.63) n_{e_\infty}^2 d / C_{e_\infty} (m_e/m_i) \ln\Lambda_\infty / T_{e_\infty}^{3/2}$$

$$a = K_{e_\infty}/C_{e_\infty}kd$$

From Eq. (1) evaluated either upstream or downstream of a plane shock where the gradients vanish, the electron energy equation reduces to a balance between electron-ion collisional energy transfer and recombination energy transfer. This balance is given by

$$\xi_{ei} + q_e = 0 \quad (5)$$

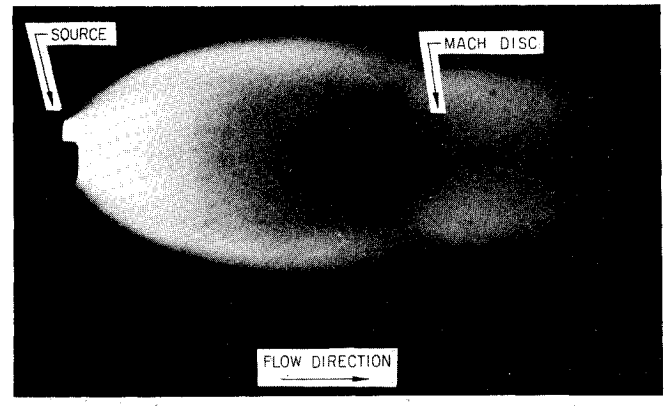

Fig. 8 Photo of freejet.

This equation will be used to complete the boundary conditions on the electron temperature. In dimensionless form Eq. (5) becomes

$$b\theta^3(\theta - \phi) = c\nu^3\epsilon(\nu) \quad (6)$$

In evaluating the constants c and b, the following conditions for the nozzle-expanded flow upstream of the shock were used:

$$M_\infty = 1.97,\ u_{e_\infty} = 1.1 \times 10^5 \text{ cm/sec}$$

$$n_{e_\infty} = 5.5 \times 10^{12} \text{ cm}^{-3},\ d = 3.68 \text{ cm}$$

$$T_{e_\infty} = 1380°\text{K},\ T_{a_\infty} = T_e = 1000 °\text{K}$$

The number density and atomic temperature downstream of the shock were assumed to obey the Rankine-Hugoniot conditions. In calculating the boundary conditions from Eq. (6) the theory of Chen[10] was used for $\epsilon(\nu)$. Chen's results, for the optically thin case, give $\epsilon = 1.42$ ev/recombination ahead of the shock and $\epsilon = 1.685$ behind it. From Eq. (6) upstream of the shock, with $\nu = 1$, $\theta_1 = 1.03$, and downstream of the shock, with $\nu = 2.25$, $\theta_2 = 1.674$. If our chosen upstream values of the flow parameters had been precisely correct, then of course the upstream value θ_1 would have come out to be unity.

The electron energy equation may be written as

$$\frac{3}{2}\frac{d\theta}{d\xi} - \frac{\theta}{\nu}\frac{d\nu}{d\xi} - a\frac{d}{d\xi}\left(\theta^{5/2}\frac{d\theta}{d\xi}\right) = -\frac{3}{2}\frac{b\nu^2(\theta - \phi)}{\theta^{3/2}} + \frac{3}{2}\frac{c\nu^3\epsilon(\nu)}{\theta^{9/2}} \quad (7)$$

In evaluating the conduction term, the value of the electron thermal conductivity appropriate to a fully ionized gas, as given by Spitzer,[21] has been used. All of the terms in Eq. (7) are included in the integration. The unknown quantities are θ, ν, and ϕ. An emperical fit to the measured ion number density distribution was constructed. Likewise, the unknown ion temperature ϕ is assumed to follow the same spatial distribution as the ion number density but to have the Rankine-Hugonoit conditions as limiting values. Using these assumed forms for ν and ϕ, Eq. (7) was numerically integrated on a CDC 6400, using a four-point Runge-Kutta scheme. The results are shown in Fig. 9.

Comparing the experimental data with the computed results, we notice that the experimental and the theoretical electron temperature increases through the shock wave are in reasonable agreement, although the experimental profile has a somewhat steeper slope. In view of the uncertainties inherent in the calculation, the agreement between theory and experiment can be considered quite good. These uncertainties include the effects of shock wave curvature, radial gradients in the flow, and the use of the optically thin values for $\epsilon(\nu)$. It can be shown that for the conditions of the ex-

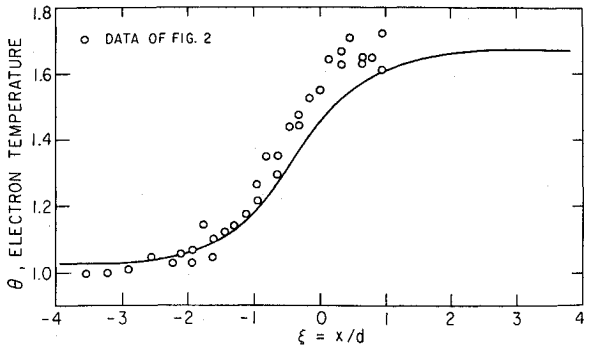

Fig. 9 Shock structure with recombination energy transfer.

periment the resonance photon mean free path is actually small compared to the plasma dimension, but because of the diffusion and escape of resonance radiation the $\epsilon(\nu)$ values, although greater, should nevertheless be close to the optically thin values. The proper values for $\epsilon(\nu)$ would be extremely difficult to determine, however.

Experimental data on the fraction of ionization energy given to the electron gas in the recombination process are scarce. Shock waves of the type encountered in this work could possibly be used to study this recombination phenomenon.

8. Conclusions

A laboratory experiment and a computer experiment on the problem of the shock structure in a partially ionized gas have been made.

The theoretically predicted elevated electron temperature in front of the shock and the electric field in the interior of the shock have been measured using the free molecule Langmuir probe as the primary diagnostic tool. The experimental data coupled with the collisional-radiative model of recombination have been used to provide an explanation of the dark space often observed in front of plasma shocks.

The electron energy equation including the effect of recombination energy transfer has been numerically integrated. A comparison of the data with the results of the integration shows substantial agreement.

References

[1] Grewal, M. S. and Talbot, L., "Shock Structure in a Partially Ionized Gas," *Journal of Fluid Mechanics*, Vol. 16, 1963, pp. 573–594.

[2] Jaffrin, M. Y., "Shock Structure in a Partially Ionized Gas," *The Physics of Fluids*, Vol. 8, 1965, pp. 606–625.

[3] Christiansen, W. H., "Study of Shock Waves in a Non-equilibrium Plasma," *The Physics of Fluids*, Vol. 10, 1967, pp. 2586–2595.

[4] Sonin, A. A., "The Behaviour of Free Molecule Cylindrical Langmuir Probes in Supersonic Flows and Their Application to the Study of the Blunt Body Stagnation Layer," Rept. 109, 1965, Univ. of Toronto Institute for Aerospace Studies.

[5] Kamimoto, G., Nishida, M., and Yoshida, K., "The Behaviour of the Charged Particles across the Normal Shock Wave in a Partially Ionized Gas," Cp. 17, Current Papers, 1967, Dept. of Aeronautical Engineering, Kyoto Univ.

[6] Peterson, E. W., "The Response of Free Molecule Cylindrical Langmuir Probes in a Turbulent Plasma," Ph.D. thesis, Aeronautical Science Report AS-68-8, 1968, Univ. of California, Berkeley.

[7] Ashkenas, H. and Sherman, F. S., "The Structure and Utilization of Supersonic Free Jets in Low Density Wind Tunnels," *Rarefied Gas Dynamics*, edited by J. H. deLeeuw, Academic Press, New York, 1966, Vol. II, pp. 84–105.

[8] Sherman, F. S., "A Source-Flow Model of Viscous Effects in Hypersonic Axisymetric Free Jets," *Archiwum Mechanilsi Stosowanej*, Vol. 2, 1964, p. 16.

[9] Hinnov, E. and Hirschberg, J. G., "Electron-Ion Recombination in Dense Plasmas," *The Physical Review*, Vol. 125, 1962, pp. 795–801.

[10] Chen, C. J., "Partition of Recombination Energy in the Decaying Rare Gas Plasmas," *The Physical Review*, Vol. 163, 1967, pp. 1–7.

[11] Loeb, L. B., *Basic Process of Gaseous Electronics*, University of California Press, Berkeley and Los Angeles, 1955.

[12] Chen, F. F., "Electric Probes," *Plasma Diagnostic Techniques*, edited by R. H. Huddlestone and S. L. Leonard, Academic Press, New York, 1965, pp. 113–199.

[13] Laframboise, J. G., "Theory of Spherical and Cylindrical Langmuir Probes in a Collisionless, Maxwellian Plasma at Rest," Rept. 100, 1966, Univ. of Toronto Institute for Aerospace Studies.

[14] Kirchhoff, R. H., "An Experimental Study of the Shock Structure in a Partially Ionized Gas," Ph.D. thesis, Aeronautical Science Report AS-69-8, 1969, Univ. of California.

[15] Kirchhoff, R. H., Peterson, E. W., and Talbot, L., "An Experimental Study of the Cylindrical Langmuir Probe Response in the Transition Regime," Aeronautical Science Report AS-69-13, 1969, Univ. of California.

[16] Kaufman, A. N., "Dissipative Effects," *Plasma Physics in Theory and Application*, edited by W. B. Kunkel, McGraw-Hill, New York, 1966, pp. 92–117.

[17] Robben, F. and Talbot, L., "Measurement of Shock Wave Thickness by Electron Beam Fluorescence Method," *The Physics of Fluids*, Vol. 9, 1966, pp. 633–644.

[18] Fraser, R. B., "Diagnostics in a Low Density Induction Heated Supersonic Plasma Flow," Ph.D. thesis, Aeronautical Science Report AS-70-5, 1970, Univ. of California.

[19] Sinclair, M., Sonin, A. A., and deLeeuw, J. H., "Diffusive Separation of Ions and Atoms in a Shock Wave," *The Physics of Fluids*, Vol. 10, 1967, pp. 891–893.

[20] Holt, E. H. and Haskell, R. E., *Foundations of Plasma Dynamics*, Macmillan, New York, 1965.

[21] Spitzer, L., *Physics of Fully Ionized Gases*, 2nd ed., Interscience, New York, 1967.